POISSON: Protostellar Optical-Infrared Spectral Survey On NTT

Simone Antoniucci[a], Brunella Nisini[a], Rebeca García López[b], Alessio Caratti o Garatti[b], Teresa Giannini[a], Dario Lorenzetti[a], Sylvie Cabrit[c], Jochen Eislöffel[d], Francesca Bacciotti[e], Tom Ray[f]

a) INAF - Osservatorio Astronomico di Roma, Monte Porzio Catone, Italy; b) Max Planck Institut für Radioastronomie, Bonn, Germany; c) LERMA - Observatoire de Paris, France; d) Thüringer Landessternwarte Tautenburg, Germany ;e) Dublin Institute for Advanced Studies, Ireland

Survey

✓ **POISSON** is a **spectral survey of Young Stellar Objects** based on ESO-NTT SofI+EFOSC2 low-resolution data covering the **wavelength range 0.6–2.4 μm**.
✓ Total sample composed of about 150 Spitzer-selected Class I and Class II sources with m_K < 12 and SED spectral index $\alpha_{2\text{-}24\mu m}$ > −1. located in five different star-forming regions: **Chamaeleon I, Chamaeleon II, L1641, Lupus, and Serpens**.
✓ Main aim of the project is to investigate accretion in YSOs by using emission features detected in the spectra.

Sample

✓ Most **sources** already **well characterised** in the literature (Cha I, ChaII: *Luhman 2004, 2007, Alcalà+ 2008, Spezzi+ 2008*; Lup: *Alcalà+ 2013, Merin+ 2008*; Ser: *Winston+ 2009*). Conversely, we characterised L1641 objects (*Caratti o Garatti+ 2012*).
✓ Range of masses: 0.1-3.0 $M_\odot$. Sub-samples also differ in mean age and extinction.

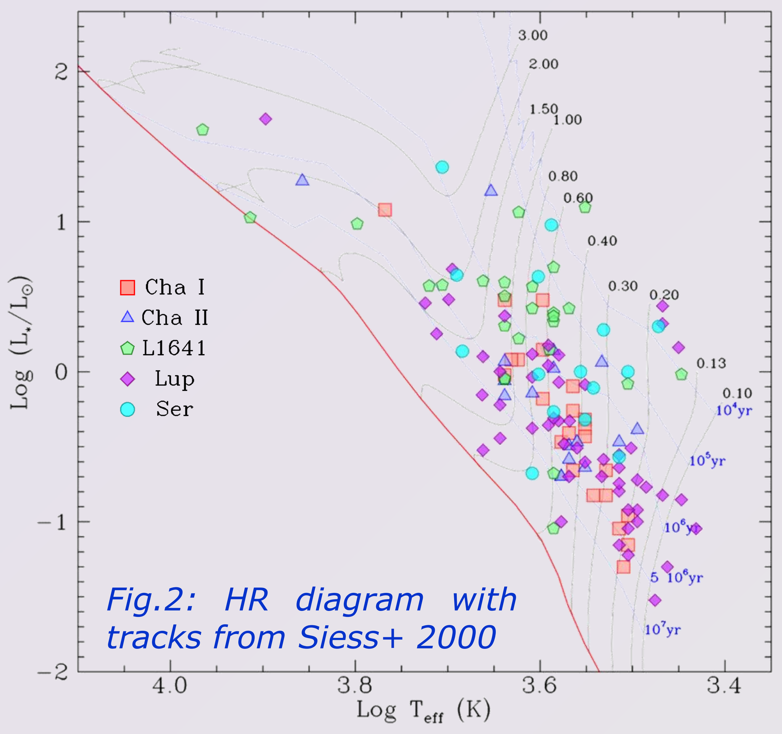

Fig.2: HR diagram with tracks from Siess+ 2000

Cha I (30objects) *(Antoniucci+ 2011)*
M_*=0.1-2.0 M_{sun}, ages=few 10^6 yr, low visual extinctions (A_V<5 mag)
Cha II (17 objects) *(Antoniucci+ 2011)*
M_*=0.1-2.0 M_{sun}, ages=few 10^6 yr, low visual extinctions (A_V<5 mag)
L1641 (27 objects) *(Caratti o Garatti+ 2012)*
M_*=0.4-3.0 M_{sun}, ages=10^5-10^7 yr, high visual extinctions (Av~10-20 mag)
Lup (54 objects) *(Antoniucci+ 2013)*
M_*=0.1-2.7 M_{sun}, ages=1-10 Myr, low visual extinctions (Av <3 mag)
Ser (18 objects) *(Antoniucci+ 2013)*
M_*=0.2-1.1 M_{sun}, ages < 3 Myr, very high visual extinctions (Av >10-30 mag)

Spectra

✓ Low-resolution (R=700÷900) spectra acquired with **EFOSC2** grism16 (OPT) and **SofI** blue and red grisms (BG, RG).
✓ Several optical/NIR **emission lines in covered range**, e.g. HI (Hα, Paβ, Brγ), [OI], CaII, HeI, [FeII], which trace accretion and ejection.
✓ RG spectrum for all objects. BG and OPT spectra not available for fainter/more embedded sources. Observing runs completed: OPT spectra of Lup and Ser could not be acquired due to bad weather.

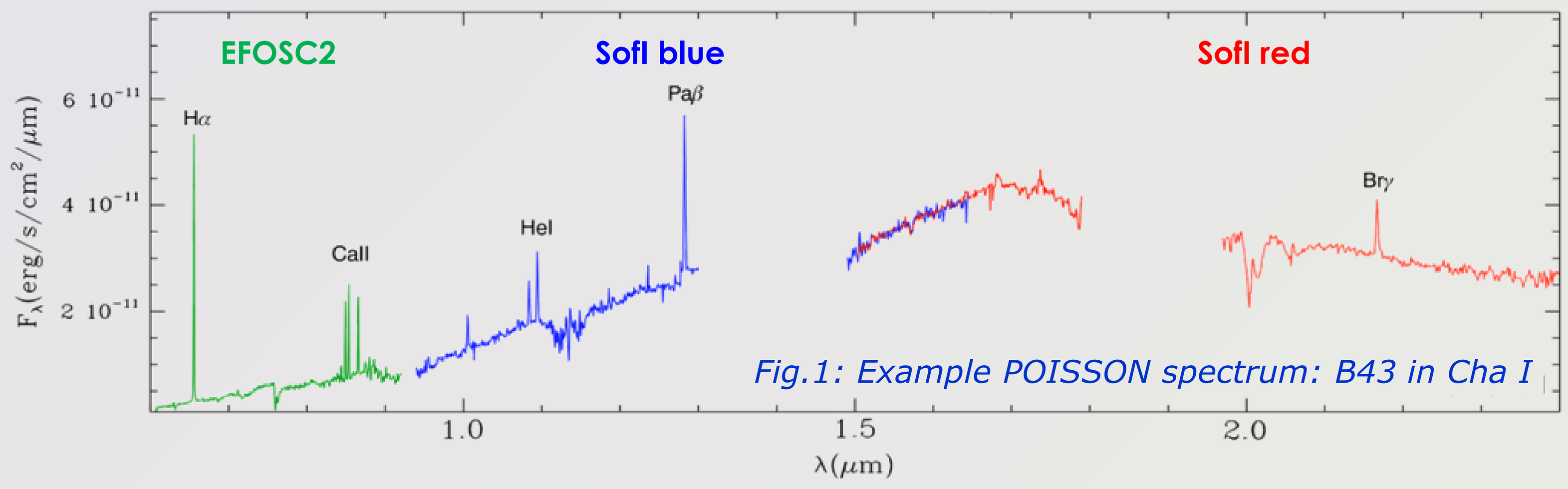

Fig.1: Example POISSON spectrum: B43 in Cha I

Emission Lines

Detection statistics for the main emission features

	[OI] 0.63μm	Hα 0.65μm	CaII 0.85μm	HeI 1.08μm	Paβ 1.μm	H_2 2.12μm	Brγ 2.16μm
Cha I	9/18	18/18	10/18	13/21	18/21	2/30	26/30
Cha II	6/15	15/15	7/15	4/16	11/16	1/17	16/17
L1641	6/14	11/14	8/14	9/16	11/16	8/27	26/27
Lup	-	-	-	18/53	26/53	4/53	21/53
Ser	-	-	-	0/4	2/4	1/18	6/18
	21/47	44/47	25/47	44/110	68/110	16/144	95/144
	45%	94%	53%	40%	62%	10%	66%

✓ Same S/N for all subsamples, so detection rates are comparable.
✓ Most prominent and numerous features detected are **HI recombination lines**.
✓ Only **few detections of** H_2 lines and other **winds/jets line tracers** (as [FeII]), likely due to sensitivity. In any case, at least 45% of objects show forbidden emission of [OI] usually associated with jets.
✓ CO and NaI emission (associated with circumstellar discs, e.g. *Najita+ 1996*) observed only in two sources.

Accretion Luminosity

Fig.3: L_{acc} values for chosen accretion tracers plotted as a function of L_*. The solid and dashed lines show the locus where L_{acc}= L_* and L_{acc} =0.1 L_*, respectively.

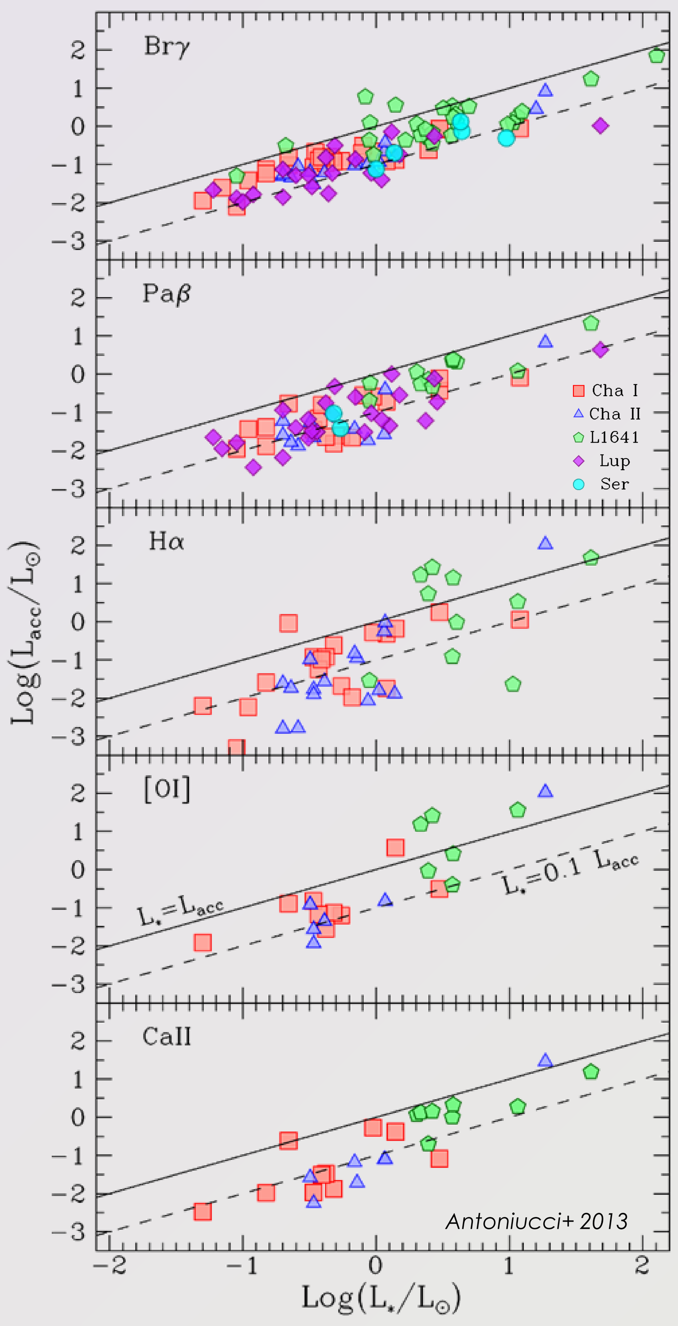

✓ Large spectral coverage allows simultaneous observation of several optical-NIR emission lines.
✓ **Accretion luminosity** (L_{acc}) of sources was **derived by using empirical relationships** available in the literature, which **connect the line luminosity to** L_{acc}. These relationships were calibrated (mostly on Taurus objects) using independent methods to measure L_{acc} (e.g. *UV-B* excess emission).
✓ **Five tracers** considered *(and relative empirical relationship)*: **[OI] λ6300** *(Herczeg & Hillenbrand 2008)*, **Hα** *(Fang+ 2009)*, **CaII λ8542** *(Dahm 2008)*, **Paβ** *(Calvet+ 2000)*, **Brγ** *(Calvet+ 2004)*.

✓ All tracers show that **L_{acc} correlates with L_*** .
✓ Tracers actually give different results for many targets.
✓ Plus, **L_{acc} determinations** present very **different scatters** for similar values of L_*
✓ **Brγ shows the smallest dispersion** (basically (0.1 L_*< L_{acc} < L_* in all range of L_*); other lines display larger scatters, up to 3 orders of magnitude (Hα).
✓ **Large L_{acc} dispersions** observed for tracers like Hα and [OI] are maybe **caused by different (variable) contributions to the lines**, e.g. winds/jet (spatially extended emission falling into slit) and chromospheric emission.
✓ Such variable contributions might have been present also in the data used to calibrate the relationships: handle with care!
✓ IR tracers are also less affected by uncertainties on extinction estimates.
✓ **Brγ** appears as the tracer **least subject to biases**, so we **adopted L_{acc} values derived from this line**.

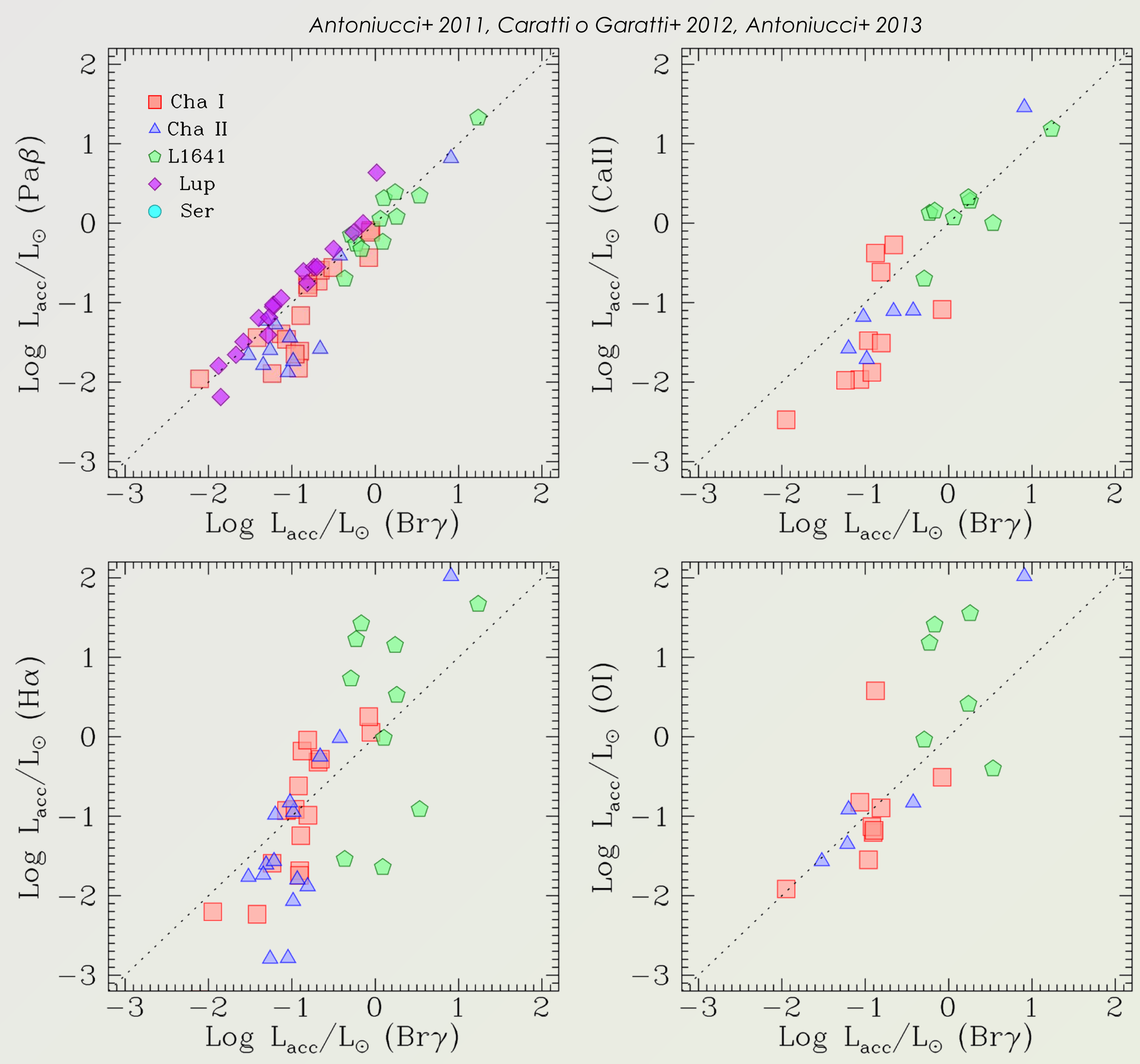

Fig.4: Direct comparison of L_{acc} determinations from Brγ and those from the other tracers. The dashed line marks the locus of equal L_{acc}.

Fig.5. L_{acc} (derived from Brγ) plotted versus the disc luminosity. The dashed line marks the locus of equal luminosity.

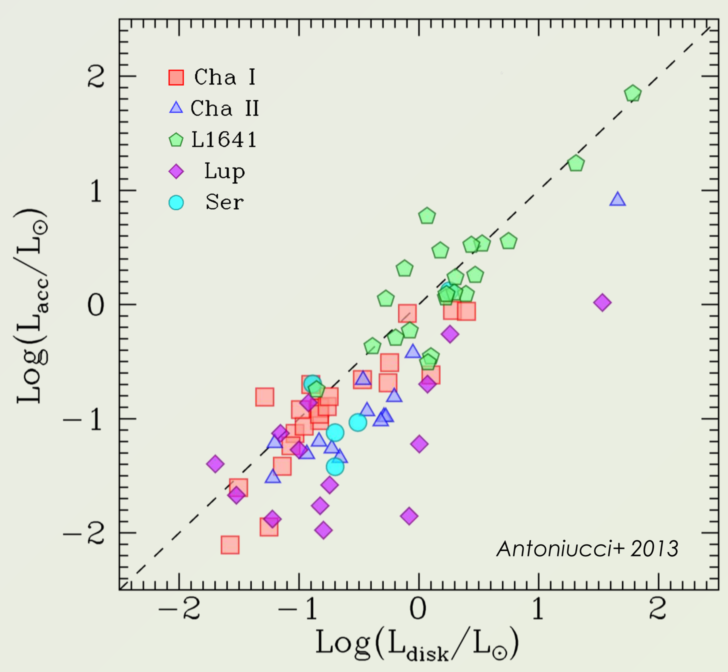

✓ In many sources L_{acc} is substantially equal to disc luminosity, which we computed as (L_{bol} − L_*).
✓ Some more evolved sources (as e.g. in Lup) show low accretion luminosities compared to the disc luminosity.

Mass Accretion Rate Relationships

✓ From L_{acc} and stellar parameters we derive the mass accretion rate ($\dot{M}_{acc}$) (e.g. *Gullbring+ 1998*). To minimise systematic biases we recomputed **mass estimates** for all sources **using the same pre-MS evolutionary tracks** *(Siess+ 2000)*.
✓ Median $\dot{M}_{acc}$ values *(L1641 > Ser > Cha I > Cha II > Lup)* reflect different mean ages of the clouds.
✓ **$\dot{M}_{acc}$ shows clear dependence on both M_* and age.**
✓ **$\dot{M}_{acc}$ ~ M_*^2**, although scatter is rather big
✓ $\dot{M}_{acc}$ variation with age is in general agreement with predictions of **$\dot{M}_{acc}$ evolution in a viscous disk** *(Hartmann+ 1998)*: (for *t* > ~1 Myr) a trend **$\dot{M}_{acc}$ ~ $t^{-\eta}$** is expected (with *η* ~ −1.5).

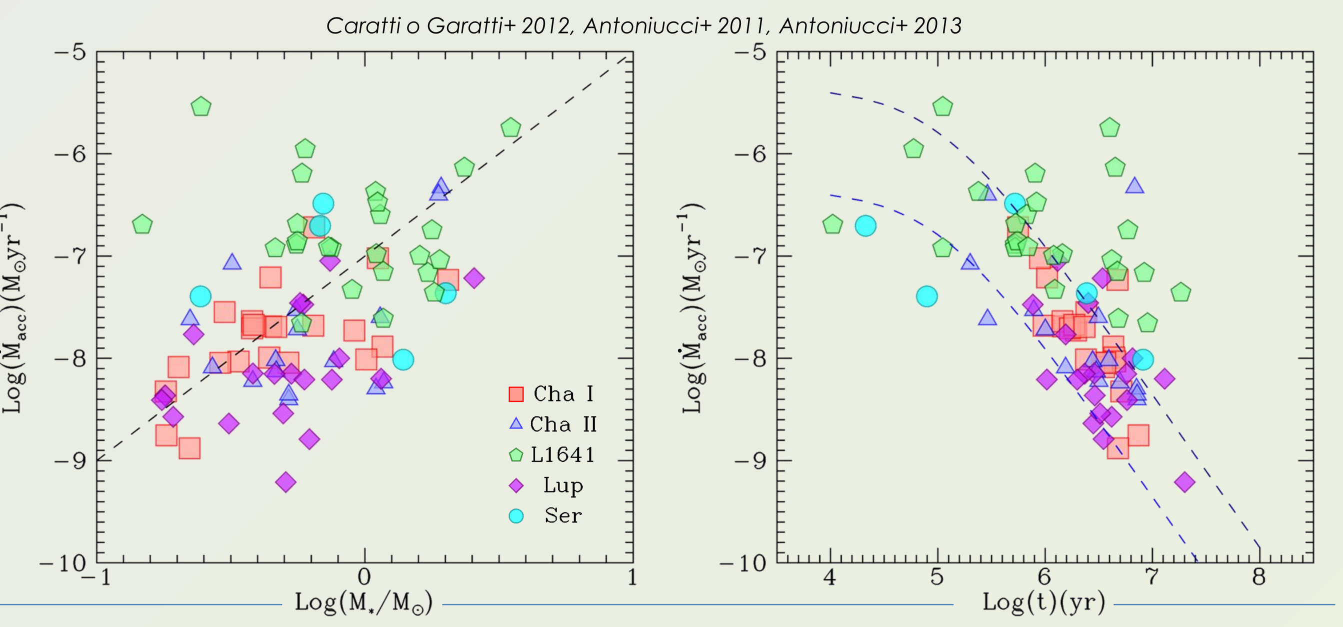

Fig.5: $\dot{M}_{acc}$ as a function of the stellar mass (left) and age of the source (right). $\dot{M}_{acc}$ shows a global trend ~ M_*^2 (dashed line). $\dot{M}_{acc}$ evolution with time is compared with predictions of viscous disc models (Hartmann+ 1998); shown dashed lines consider a viscosity parameter α=0.01 (constant for all disc radii) and different stellar and disc masses: M_* =0.5 $M_\odot$, M_D =0.1 $M_\odot$ (lower line) M_* =1.0 $M_\odot$, M_D = 0.5 $M_\odot$ (upper line).

✓ To better analyse $\dot{M}_{acc}$ dependence on M_* and age we **normalise $\dot{M}_{acc}$ by $t^{-\eta}$** and **by M_*^{β}**, respectively, using a procedure in which we simultaneously fit the normalised datasets to get the best-fit power indexes (*η*, *β*) of the relationships.

Normalise by $t^{-\eta}$ Normalise by M^{α}

✓ Correlations appear tighter when considering normalised data.
✓ Stellar mass: best-fit provides **$\dot{M}_{acc}$ ~ $M_*^{2.2 \pm 0.2}$**. Dependence on mass is similar to the one observed in other low-mass star-forming regions: ~$M_*^{1.8}$ *(Natta+ 2004)*, ~$M_*^{2.8}$ *(Fang+ 2009)*, ~$M_*^{1.9}$ *(Herczeg & Hillenbrand 2008)*, ~$M_*^{2.1}$ *(Muzerolle+ 2005)*, ~$M_*^{1.6}$ *(Rigliaco+ 2011)*.
✓ Age: best-fit (for Log *t* > 5.9) gives **$\dot{M}_{acc}$ ~ $t^{-1.6 \pm 0.2}$**. Observed spread may be due to spread of initial disk masses, presence of outbursting objects, and different viscosity laws (e.g. *Isella+ 2009*). Evolution is faster than found in other works (e.g. $t^{-1.2}$, *Sicilia-Aguilar+ 2010*): faster dissipation is actually consistent with scenarios in which additional processes contribute to disk dissipation, such as photoevaporation (e.g. *Gorti+ 2009*).

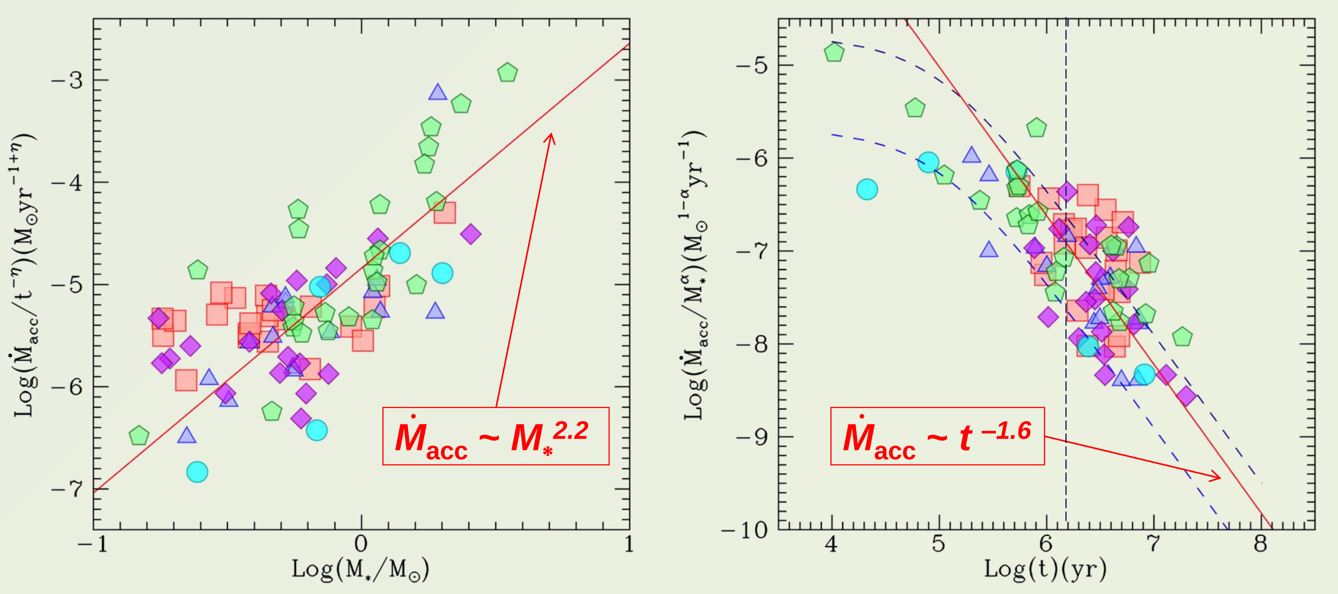

Fig.6: As in previous Fig.5 but for normalised quantities $\dot{M}_{acc}$ /$t^{-\eta}$ (left) and $\dot{M}_{acc}$ /M_*^{β} (right), where η=1.6 and β=2.2, which are the best-fit power indexes. Best-fit lines are shown in red. The fit for $\dot{M}_{acc}$ /M_*^{β} is performed only with points having Log(t)>5.9 (dashed vertical line), where the expected time evolution is described by a simple power law.

simone.antoniucci@oa-roma.inaf.it

REFERENCES: Alcalà et al. 2008, ApJ, 676, 427; Alcalà et al. 2013, in prep.; Antoniucci et al. 2011, A&A, 534, 32; Antoniucci et al. 2013, A&A, in prep.; Calvet et al. 2000, PPIV, 377; Calvet et al. 2004, AJ, 128, 1294; Caratti o Garatti et al. 2012, A&A, 538, 64; Dahm 2008, AJ, 136, 521; Fang et al. 2009, A&A, 504,461; Gorti et al. 2009, ApJ, 705, 1237; Gullbring et al. 1998, ApJ, 492, 323; Herczeg & Hillenbrand 2008. ApJ, 681, 594; Isella et al. 2009, ApJ, 701, 260; Luhman 2007, ApJSS 173, 104; Luhman 2004, Apj 602, 816; Merin et al. 2008 ApJS, 177, 551; Muzerolle et al. 2005, ApJ 625, 906; Najita et al. 1996, ApJ, 462, 919; Natta et al. 2004, A&A, 452, 245; Rigliaco et al. 2011 , A&A, 525, 47; Sicilia-Aguilar et al. 2010 , ApJ, 710, 597; Siess et al. 2000, A&A, 358, 593; Spezzi et al. 2008, ApJ 680, 1295; Winston et al. 2009, AJ, 137, 4777.